JOURNAL OF MATERIALS SCIENCE 27 (1992) 6116–6122

X-ray differential line broadening on tabular haematites

G. M. DA COSTA, M. F. DE JESUS FILHO*
Departamento de Química, Universidade Federal de Minas, Gerais, 31270 – Belo Horizonte, MG, Brazil

The haematites obtained by dehydration of three synthetic goethites of different sizes have been characterized by X-ray diffraction, Mössbauer spectroscopy and transmission electron microscopy. The transformation itself has been studied by thermogravimetric analysis and differential scanning calorimetry. Samples (24) obtained by annealing the goethites for 30 min at several temperatures up to 900 °C were analysed. All samples had a tabular shape. The variation of the internal magnetic field, as well as of the line widths of the spectra at room temperature, indicate growth of the particle size. The constant value for the quadrupole splitting and the absence of a distribution of hyperfine interactions of the spectra at 80 K excluded the presence of iron ions out of their normal positions. No strain was detected by X-ray diffraction. The results also showed a differential line broadening in the haematite pattern, but there was no shift in the position of the lines. This broadening was present in all lines, including those wih $l = 3n$ ($n = 0,1,2,\ldots$). Increasing the treatment temperature made all lines sharp. The relative integrated intensities, $I(1\,1\,0)/I(1\,0\,4)$, of each series remained unaltered, but the relative intensities did not. The above results lead to the conclusion that the differential X-ray line broadening of haematites derived from goethite occurs only in tabular (or acicular) haematites with small size. For small spherical particles, the broadening should be uniform for all lines.

1. Introduction

The transformation of goethite to haematite has been extensively studied in recent years. It is well known that crystals of goethite give rise to haematite with the same shape of the initial goethite when the transformation is carried out at low temperatures, usually less than 600 °C. As the temperature of synthesis increases, the haematite crystals become nearly spherical [1–6].

Because of the close relationship between the unit cells of these two substances, the formation of haematite occurs without great disruption of the goethite structure. The a,b,c axes of the original orthorhombic cell of goethite become c,a and $(1\bar{1}0)$ directions, respectively, of the pseudohexagonal cell of haematite [2]. The orientation of the axes for a tabular haematite is given by Duvigneaud and Derie [7].

An interesting feature of haematites obtained from goethites at low temperatures is a non-uniform broadening of the X-ray diffraction lines. The powder pattern reflections with $l \neq 3n$ ($n = 0,1,2,\ldots$) are broad and become sharp on further heating; on the other hand, the lines with $l = 3n$ (or $h - k = 3n$) remain sharp. There is no displacement of any line position [6–11]. Despite several works on this problem, the interpretations of the data, to date, have been sometimes conflicting. Furthermore in these mentioned works, no study has been reported of the set of the seven principal lines of the haematite pattern, nor has any systematic heating of goethites of different initial size been performed. These points were investigated in the present work, and the results are reported, emphasising in detail the influence of the particle shape in this broadening.

2. Experimental procedure

Three goethite samples were hydrothermally synthesized by mixing 0.5 l 1.1M $Fe(NO_3)_3$ with 0.5 l 4.3M KOH. After dilution to 2.0 l while stirring for 2 min, the suspensions were stored at the temperatures and for the times shown in Table I

After the storing for the times indicated, the samples were washed three times with distilled water by centrifugation until pH $\simeq$ 7 was reached. They were dried at 110 °C for 2 h and finally were gently ground.

The goethites were heated in a porcelain dish in an electric furnace with the temperature controlled to $\pm$ 5 °C. Heating was carried out for 30 min in air and the samples were allowed to cool slowly out of the furnace.

* Author to whom all correspondence should be addressed.

0022–2461

TABLE I

Sample	Temperature (°C)	Time (days)
GD	20 ± 2	20
GE	50 ± 2	12
GF	90 ± 2	7

The samples were labelled in the following way: H refers to a heated sample; the second letter refers to the original goethite, and the number shows the treatment temperature (°C).

X-ray powder diffraction (XRD) patterns were obtained using a Rigaku–Geigerflex apparatus, CoK_{α_1} radiation, a graphite monochromator, scanning speed of 1° 2θ/min^{-1}, receiving slit of 0.15° and divergence slit of 1°. An angular step of 0.025° (2θ) was achieved and the diffractograms were recorded with the help of a microcomputer. The instrumental profile was obtained from an analytical grade α-Fe_2O_3 annealed at 1000 °C for 2 h. The integral breadth, line position and integrated intensity were obtained from fitting each peak with a Gaussian distribution by the least squares method. The correction for the instrumental broadening was made by the Gaussian approximation [12]. In order to verify the presence of strain broadening in the haematites, the development given by Klug and Alexander [12] was used with the (012) and (024) lines. The mean crystallite dimensions (MCD) were calculated using the Scherrer formula after subtracting the strain contribution. The mean crystallite sizes along the crystallographic axes (MCD_x, $x = a,b,c$) were obtained from the equation $MCD_x = MCD \cos\phi$, where ϕ is the angle between the normal to the plane and the axis under consideration.

Mössbauer spectra were taken at 80 and 293 K with the apparatus described elsewhere [13].

Transmission electron microscopic (TEM) observations were made in a Jeol Jem 200A microscope operating at 100 kV. A droplet of a solid suspension in acetone, prepared by agitation with a stick ultrasound equipment, was withdrawn and then put on a copper grid coated with a carbon film.

Thermogravimetric analysis (TGA) and differential scanning calorimetry (DSC) were performed using a Mettler TA 3000 system coupled to a TC10A processor. Samples of ≃ 20 mg, an air stream and aluminium crucibles, were used in both experiments. In the DSC analysis the heating rate was 5 °C min^{-1} and in the TGA experiment the rate was 10°C min^{-1}.

3. Results and discussion

DSC curves of some samples are shown in Fig. 1. The samples heated above 340 °C show only the surface water peak and their curves are not shown. In all samples there is a small endothermic peak between 25 and 150 °C due to the loss of chemisorbed surface water. The GD sample presents another endothermic peak at 262°C corresponding to loss of structural OH. The ΔH value, calculated by the processor, is 21.5 kJ mol^{-1}. The curves of the HD290 and HD340

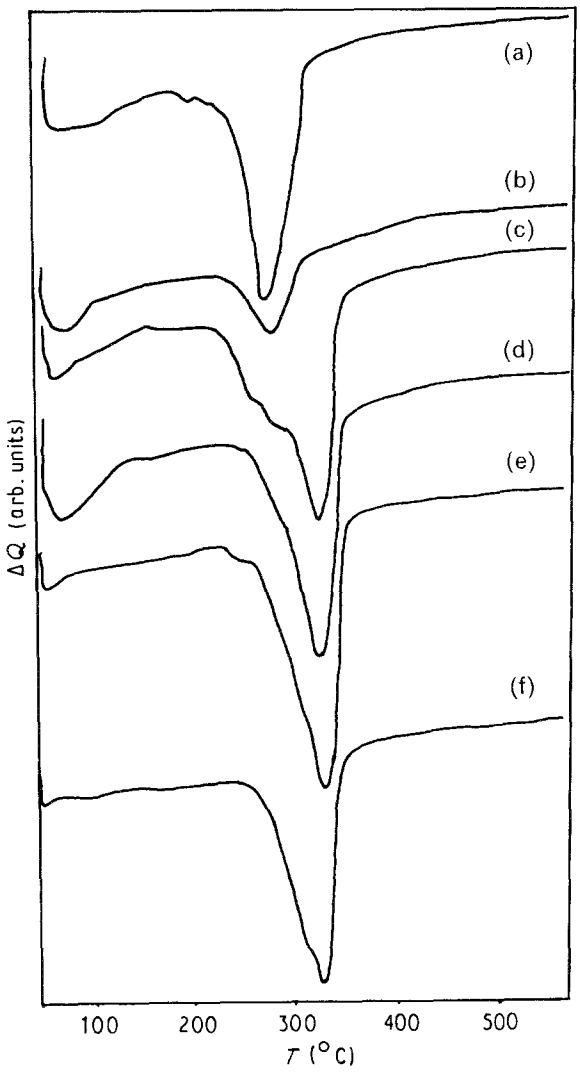

Figure 1 DSC curves for goethites D, E, F and samples heated at 340 °C. (a) GD, (b) HD340, (c) GE, (d) HE340, (e) GF, (f) HF340.

samples are similar to the GD curves, but the ΔH value for HD340 is only 6.8 kJ mol^{-1}. The GE sample shows three peaks at 259, 275 and 318 °C, with ΔH = 23.7 kJ mol^{-1}. The HE290 curve is identical, but that for HE340 shows only the higher temperature peak and the ΔH value is 17.4 kJ mol^{-1}. The GF, HF290 and HF340 samples exhibit main peaks at 322 °C and small shoulders at 245°C. The ΔH value for these samples is 24.5 kJ mol^{-1}.

Because the system is constituted only by goethite and/or haematite, we can assume that the decrease in the ΔH values of some samples is due to the previous existence of haematite. Thus, we can estimate 70% and 27%wt/wt as the amount of haematite in the HD340 and HE340 samples respectively.

The amount of chemisorbed water, calculated from TGA analysis, varies from 1.7%–3.6% wt/wt for all samples. The structural OH lost is 11.0% wt/wt for GD, 3.7% for HD340, 10.1% for GE, 7.3% for HE340, and 10.0% for the GF goethite. From these values we estimate 68% and 28% wt/wt as the amounts of haematite in the HD340 and HE340 samples, respectively.

The DSC triple peak in the GE goethite has been observed by many authors, both in synthetic and

natural samples, but until now no definitive explanation seems to have been offered. Schwertmann [14] observed a double peak and proposed the existence of two types of goethite that differ only in the *a* dimension of the unit cell. Goss [15] also observed two (or more) peaks and said that they were due to non-stoichiometric amounts of water, while Patterson and Swaffield [16] believed in the existence of surface hydroxyl groups singly, doubly and triply co-ordinated. The approximated area of the two low-temperature peaks in the GE sample is between 25% and 35%, with 28% haematite in the HE340 sample. Remembering that there is only a higher temperature peak in the latter sample, it is reasonable to assume that the low-temperature peaks in the GE sample are due to the loss of structural OH and not to the loss of surface water. The appearance of multiple peaks is here attributed to the distribution of particle sizes, in accordance with the Mössbauer results [13].

Because no other peak was found in any sample, we concluded that there is no recrystallization process involved when the samples are heated to 600 °C. This result agrees with the experiments of Goss [15] and Schwertmann [14]. However, Goni-Elizalde and Garcia-Clavel [17] observed an exothermic peak near 500 °C and attributed it to an improvement in the haematite crystallinity.

Fig. 2 shows XRD patterns of the goethites. The line positions are consistent with the JCPDS card [18]. It was not possible to test the presence of strain due to the low number of statistics for the (020) and (040) lines (the (020) is not shown in Fig. 2). Assuming that all broadening is caused by the small crystallite size, we found the mean dimensions shown in Table II. As can be seen, the GD goethite is the smallest, while the GE and GF have almost the same sizes. At 290 °C there is no detectable modification.

The XRD patterns of haematite of the D, E and F series are very similar; Fig. 3 shows the diffractograms of the D series. The HD340 sample contains a mixture of haematite and goethite, the same occurring in the HE340. In all other samples only haematite is present. No shift of line position is seen throughout the series,

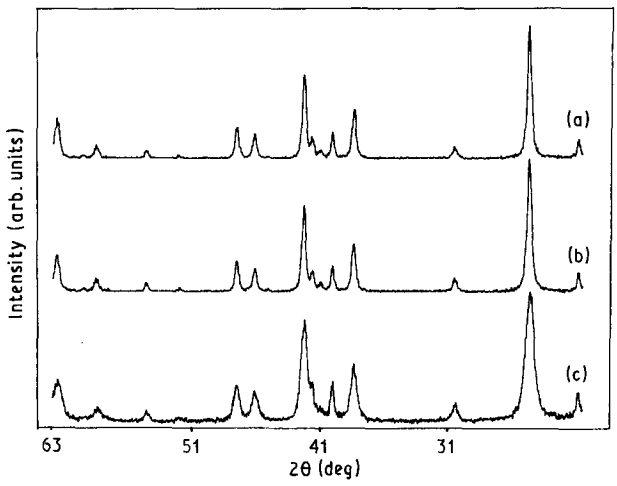

Figure 2 X-ray diffractogram patterns of goethites. (a) GF, (b) GE, (c) GD.

TABLE II Mean crystallite dimensions in *a* and *b* directions of goethites. MCD_b was calculated from the (021) plane. MCD_a is the mean value of (140), (130), (110) and (111) planes for GD, GE and GF samples; for the others, MCD_a is the mean of (140), (111) and (130) planes

Sample	MCD_a (nm)	MCD_b (nm)
GD	12.0 ± 1.6	18.5
HD290	11.6 ± 2.2	17.2
GE	20.4 ± 2.2	26.2
HE290	19.7 ± 2.0	24.7
GF	23.2 ± 3.6	28.2
HF290	22.0 ± 3.7	28.4
HF340	21.8 ± 3.3	23.6

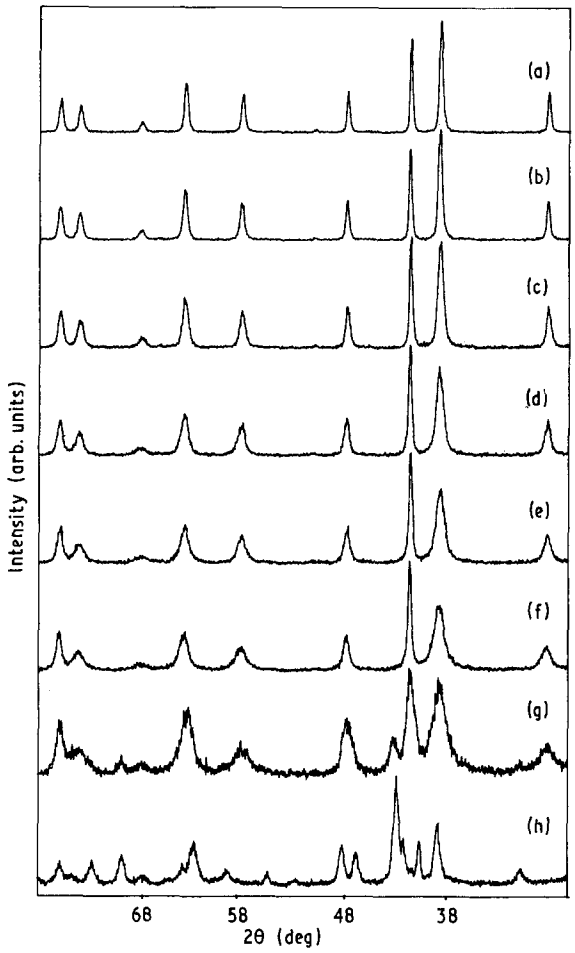

Figure 3 X-ray diffractogram patterns of series D haematites. (a) HD900, (b) HD800, (c) HD710, (d) HD620, (e) HD530, (f) HD440, (g) HD340, (h) GD.

all positions being in accordance with the JCPDS card [18]. It is very evident that a notable inversion occurs in the intensities of the (110) and (104) lines, but the integrated intensities remain constant, as shown in Fig. 4. The presence of strain was checked using the (012) and (024) lines, but it was found to make a small or non-existent contribution to the broadening.

The mean crystallite sizes in the *a* and *c* directions are shown in Tables III–V. Values for HD340 and HE340 samples were not calculated due to the superposition of some goethite and haematite lines.

Fig. 5 shows electron micrographs of some selected samples. From these we can infer that both goethite

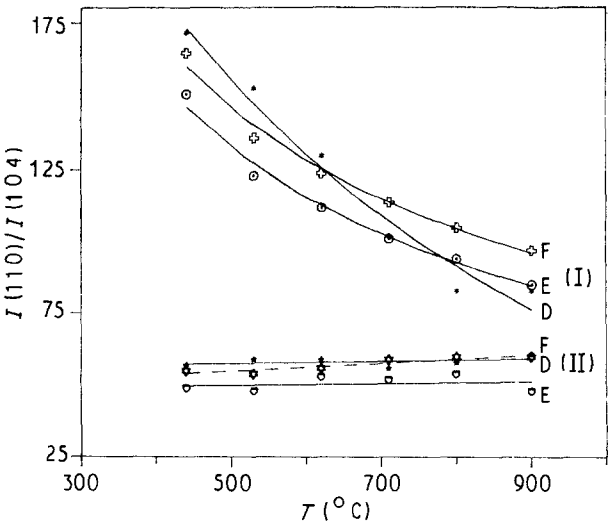

Figure 4 Ratio of the intensities and integrated intensities of (110) and (104) haematite lines. (I) intensities; (II) integrated intensities.

TABLE III Mean crystallite dimensions in *a* and *c* directions for series D haematites. MCD_a is the mean value of (110) and (300) planes; MCD_c of the planes (116) and (113); MCD_c^* include (012), (024) and (104) planes.

Sample	MCD_a (nm)	MCD_c (nm)	MCD_c^* (nm)
HD340	11.9 ± 1.3	6.4 ± 1.0	5.1 ± 1.3
HD440	25.3 ± 1.7	9.1 ± 0.2	7.3 ± 1.6
HD530	25.9 ± 2.9	9.7 ± 0.3	8.5 ± 1.1
HD620	27.2 ± 3.2	11.0 ± 0.3	9.9 ± 1.2
HD710	30.8 ± 2.8	14.1 ± 0.9	13.0 ± 1.7
HD800	36.4 ± 2.4	18.7 ± 1.6	18.3 ± 2.2
HD900	42.4 ± 5.0	23.3 ± 2.2	22.3 ± 2.9

TABLE IV Mean crystallite dimensions in *a* and *c* directions for series E haematites. MCD_a is the mean value of (110) and (300) planes; MCD_c of the planes (116) and (113); MCD_c^* include (012), (024) and (104) planes

Sample	MCD_a (nm)	MCD_c (nm)	MCD_c^* (nm)
HE440	31.3 ± 0.9	17.3 ± 0.9	11.5 ± 4.9
HE530	31.6 ± 0.1	16.4 ± 0.6	11.7 ± 4.0
HE620	31.4 ± 1.0	16.8 ± 0.5	12.2 ± 3.1
HE710	33.1 ± 0.9	15.0 ± 0.7	12.9 ± 2.2
HE800	33.5 ± 0.9	17.8 ± 0.3	14.2 ± 2.7
HE900	38.2 ± 0.4	16.4 ± 1.0	14.9 ± 1.8

TABLE V Mean crystallite dimensions in *a* and *c* directions for series F haematites. MCD_a is the mean value of (110) and (300) planes; MCD_c of the planes (116) and (113); MCD_c^* include (012), (024) and (104) planes

Sample	MCD_a (nm)	MCD_c (nm)	MCD_c^* (nm)
HF440	32.3 ± 2.7	18.8 ± 0.1	12.0 ± 5.6
HF530	31.6 ± 2.3	16.6 ± 1.3	11.8 ± 4.0
HF620	32.0 ± 1.5	16.7 ± 0.3	12.4 ± 3.7
HF710	32.2 ± 2.2	17.0 ± 0.5	13.7 ± 3.0
HF800	32.8 ± 1.9	17.2 ± 0.1	14.0 ± 3.1
HF900	34.8 ± 1.8	17.6 ± 0.5	15.4 ± 2.7
HF1000	34.6 ± 0.2	18.5 ± 0.8	16.3 ± 2.8

and haematite have an elongated form, i.e. the shape of the goethite is preserved, even in those samples heated at higher temperatures. The sizes calculated using XRD show that the widths and thicknesses (MCD_b and MCD_a for goethite, MCD_a and MCD_c for haematite) are different. Therefore, we could conclude that the particles are tabular. In addition, the presence of pores in some samples can be noted.

The Mössbauer room-temperature spectra show the following features: the internal magnetic field increases from 505 kOe (HD440) to 513 kOe (HD900); 505 kOe (HE440) to 512 kOe (HE900) and 507 kOe (HF440) to 511 kOe (HF1000); the isomer shift, 0.38 mm s^{-1} relative to metallic iron, and the quadrupole splitting, -0.22 mm s^{-1}, are constant for all samples. The line width changes from 0.60 mm s^{-1} for the samples obtained at low temperatures, to 0.52 mm s^{-1} for those obtained at higher temperatures. The variations in the internal magnetic field indicate that the particle sizes increase as the synthesis temperature is increased. This conclusion is supported by the variation in the line width. An increase in this parameter is expected when the particle size decreases to the range of sizes where superparamagnetism relaxation effects take place. All spectra show a small central doublet due to superparamagnetism, except for samples HD800 and HD900. This doublet corresponds to 1.5% of the total area for the HD440 sample and 0.5% for HD710. In series E, this superparamagnetic fraction has a maximum value, 7%, for HE440 and a minimum value, 4%, for HE900. For series F these fractions are similar to those for series E. These results are in agreement with the DSC analysis, where a broader particle-size distribution is inferred for series E. Such aspects are also present in the goethites samples.

In the Mössbauer spectra at 85 K, the internal magnetic field of the weakly ferromagnetic (wfm) phase increases from 525 kOe (low-temperature samples) to 528 kOe (high-temperature samples). For the antiferromagnetic (afm) phase the corresponding values lie between 535 and 538 kOe. The quadrupole splitting for the afm phase is 0.39 mm s^{-1} and is constant for all haematite samples; the line width is 0.30 mm s^{-1}. From these two parameters we can reject the possible presence of a distribution of hyperfine interactions. In particular, investigation of the presence of these distributions in compounds with magnetic order by Mössbauer spectroscopy is quite adequate. The sensitivity of this technique to such distributions is increased by the presence of a magnetic hyperfine interaction, compared to electrostatic interactions only [19, 20]. Moreover, the calculations of Artman *et al.* [21] show that very slight changes in the positions of iron in the haematite unit cell may lead to considerable changes in the electric field gradient at the iron site.

The absence of distributions of hyperfine interactions and the lack of variation of the quadrupole splitting leads to the conclusion that iron ions are observed as regular unpertubed sites. Therefore, the possibility that iron ions in haematite are not in their normal positions, as claimed by some authors [8] in

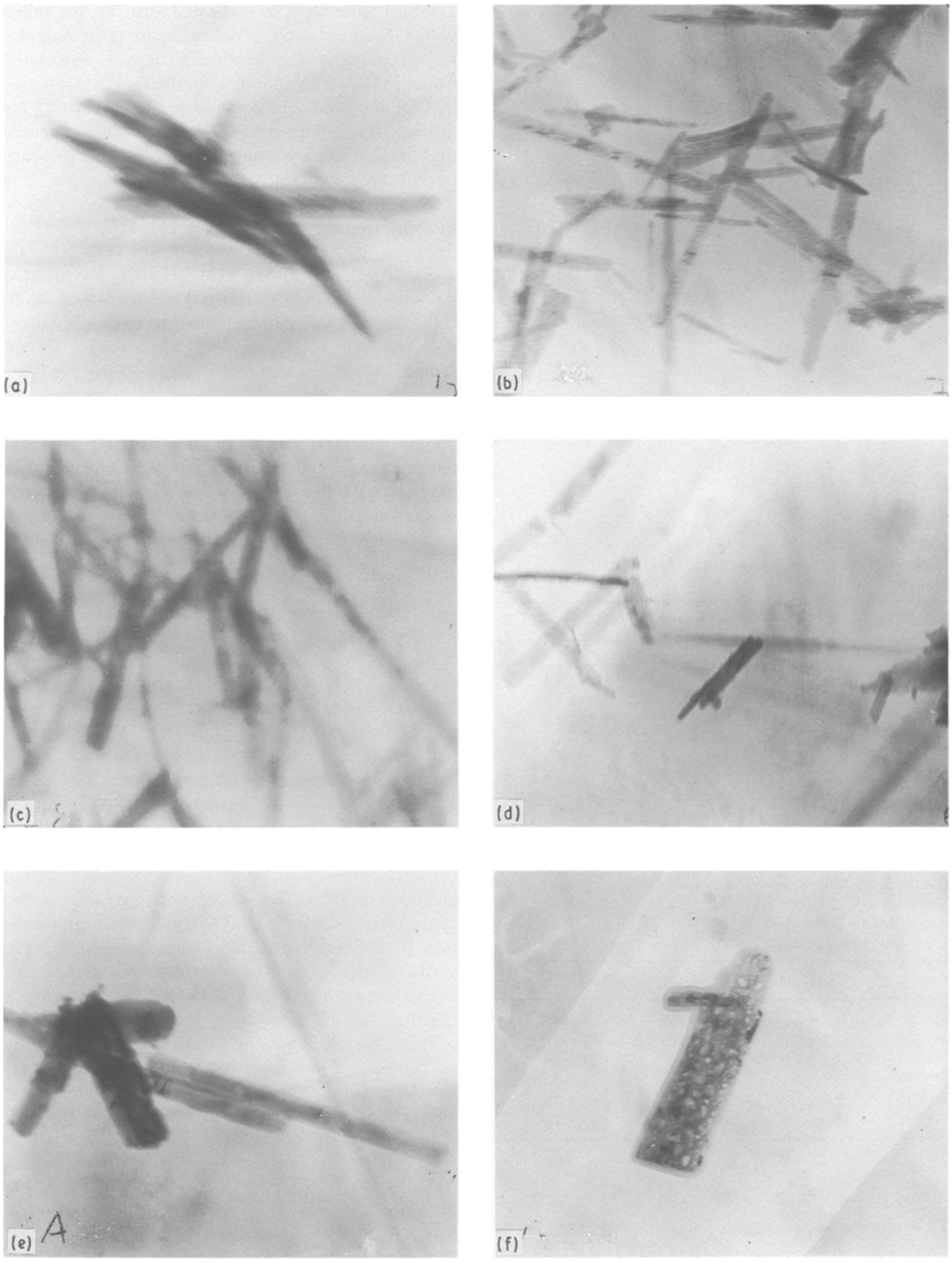

Figure 5 Transmission electron micrographs of some selected samples. (a) GF, (b) HE340, (c) HF620, (d) HE620, (e) HD620, (f) HE900.

order to explain the differential broadening of the X-ray lines, may be rejected.

From Tables II–V we can observe that series D exhibits a large growth with increase in the synthesis heating temperature. The haematite formed at 440 °C was the smallest, while that formed at 900 °C was the largest. The variation of size in the *a* direction is 68% for series D, 22% for E and only 7% for F. On the other hand, in the *c* direction these variations are 200% for series D, while for series E and F it was non-existent. Several important considerations can be drawn from the X-ray results.

1. There was no shift in the line positions.
2. The relative integrated intensities, $I(110)/I(104)$, of each series remained unaltered, but the relative intensities did not.
3. For series D, all lines are broad and became very sharp with increasing synthesis temperature.
4. For series E and F the $l = 3n$ lines were sharper than those of series D, and their integral breadth variations were less pronounced.
5. Mean crystallite dimensions in the a direction, calculated from the (110) and (300) reflections, gave a mean value with a deviation of 10%. The size calculated from (300) was always less than that for (110).
6. Mean sizes in the c direction, calculated from (116) and (113) planes, agree within 10%. Including the (012), (024) and (104) planes increases the error to 35%, but this is reduced to 15% in the higher temperature samples.
7. The $l \neq 3n$ reflections always gave smaller sizes than the $l = 3n$ reflections.

At this point it is necessary to review the different explanations that have been given to this differential X-ray line broadening. Rooksby [2] proposed the existence of a sub-unit, common both to goethite and haematite, that suffers only a little disturbance when goethite is transformed into haematite on heating. The X-ray reflections of this sub-unit are those with interplanar spacings nearly equal for goethite and haematite; these lines are sharp. This does not explain why the H(104) line ($d = 0.270$ nm) is broad, because a G(130) line with $d = 0.269$ nm exists. Lima de Faria and Gay [10] observed a non-uniform broadening in haematites obtained from fibrous natural goethite, but not in samples obtained from well-crystallized goethites. They attributed this broadening to stacking faults in the $h-k \neq 3n$ planes. On the other hand, the $l = 3n$ planes would not be affected. Nakagima *et al.* [11] also proposed that the metal sublattice is divided into small domains with stacking faults. These propositions conflict with our results because some samples presented very broad $l = 3n$ lines (see the (116) line of series D). Moreover, stacking-fault effects cause a shift in the line positions, not observed in the present work. Naono and Fujiwara [5] synthesized haematites from acicular goethites and observed slit-shaped micropores perpendicular to the c-axis of haematite. These micropores were formed in samples obtained at 300 °C; at 400–600 °C they were transformed into nearly circular pores. As the H(104) line broadening was reduced when the synthesis temperature was increased, they suggested that the micropores were the cause of the broadening. However, no correlation between the differential broadening and micropores characteristics was established. Watari *et al.* [6, 22, 23] concluded that haematites obtained from goethite are twinned, and each variant behaves in a different way. The $l = 3n$ reflections belong to the two variants and are sharp, whereas $l \neq 3n$ reflections belong to one variant and are broad. They did not observe any shift in the line positions, and the integrated intensities of the H(104) peaks are nearly constant for samples obtained between 265 and 600 °C. Watari *et al.*'s explanations [6] also disagree with our results, because some $l = 3n$ lines are very broad (see series D). Yamaguchi and Takahashi [8] associated the non-uniform broadening with an incomplete displacement of the iron atoms. On increasing the treatment temperature, these atoms reach the equilibrium lattice positions. If this is true, there would be a variation in the integrated intensities of H(104) and (110) planes. However, our results showed that this does not occur. The Mössbauer results, as discussed earlier, also elim-

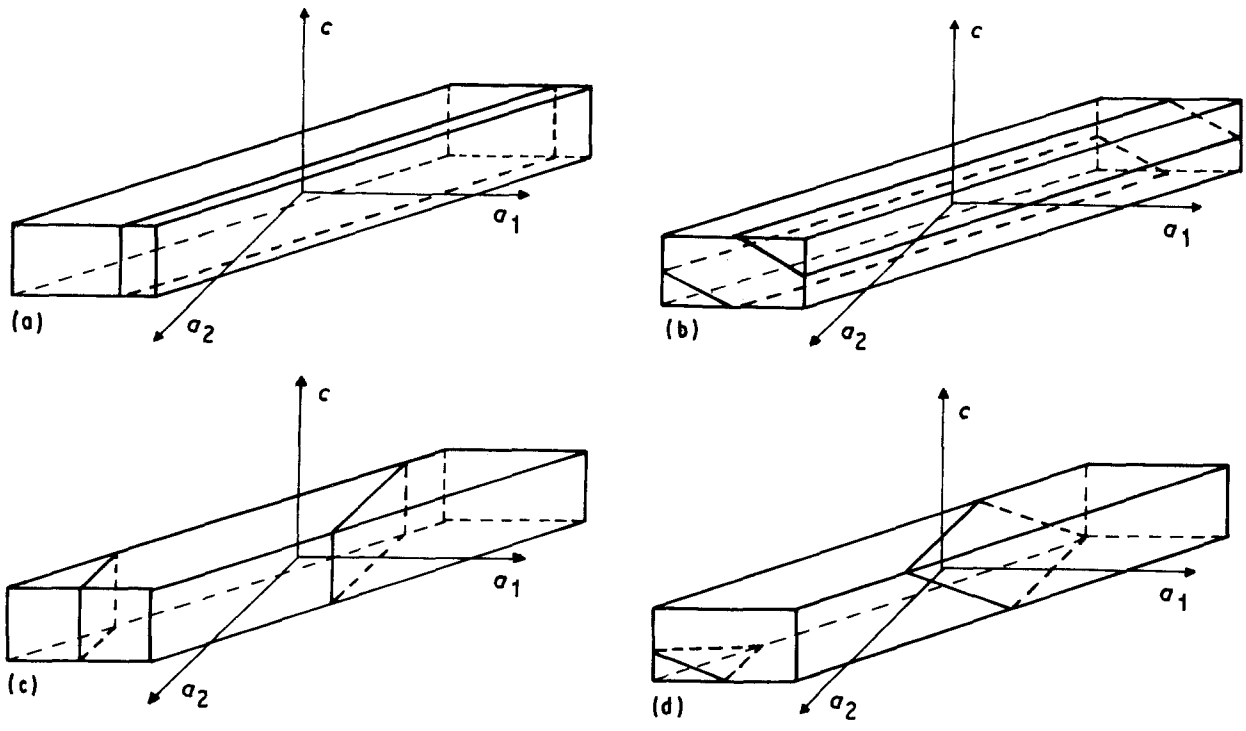

Figure 6 Schematic representation of (a) (110), (b) (116), (c) (300) and (d) (104) planes in tabular crystals of haematite.

inate the possibility of this incomplete displacement because, as shown by Artman *et al.* [21], the quadrupole splitting is very sensitive to iron vacancies [13].

In order to analyse our results in a different way, we used Fig. 6, showing (110), (300), (116) and (104) planes for a tabular haematite. Assuming a mosaic structure [6] we can observe that:

(a) all (110) planes cut several crystallites;

(b) (300) planes cut more crystallites when they are in the central region; towards the edges in the length direction, there are fewer crystallites. Thus the (300) X-ray reflection should be broader than (110);

(c) the same behaviour is observed for (116) planes, but they are limited by the depth. Towards the surface there are fewer crystallites in these planes (the same is valid for (113) planes);

(d) for (104), (012) and (024) planes, the edge limitations are still greater, because they are affected by the length as well as by the depth. There are much fewer crystallites in these planes than in $l = 3n$ planes, so their reflections should be broader than the others.

Duvigneaud and Derie [7] also observed a non-uniform broadening in haematites derived from tabular and acicular goethites, but not in those derived from spherical or ovoid goethites. A small strain contribution was also observed in the low-temperature haematites. They concluded that the broadening can be explained by anisotropy of particle shape.

In view of the above reasoning, we expect that the non-uniform broadening would occur only in tabular (or acicular) small haematites. For small spherical particles, the broadening will exist, but should be uniform for all X-ray lines.

4. Conclusions

Evidence for the broadening of the $l = 3n$ lines was clearly found. The combined effects of temperature, heating time, size and shape of the original goethite enabled the broadening to be detected. A time of 30 min was sufficient for transformation to occur without a large sintering process. Therefore, from a systematic study of different haematites, we could infer that the differential X-ray line broadening will be present only in tabular (or acicular) small haematites. Therefore, the broadening can be atributed to the specific shape associated with a small size of the haematite particles.

Acknowledgements

The authors thank Professor Eustaquio Galvão da Silva for helpful discussions, and Mr André Tenuta Azevedo, Usinas Siderúrgicas de Minas Gerais, for help with arranging the conditions for the X-ray experiments. This work was supported by CNPq and FAPEMIG.

References

1. M. H. FRANCOMBE and H. P. ROOKSBY, *Clay Minerals Bull.* **4** (1959) 1.
2. H. P. ROOKSBY, *Silicates Industriels* **25** (1960) 335.
3. J. LIMA de FARIA, *Acta Crystallogr.* **23** (1967) 733.
4. A. THRIERR-SOREL, J. P. LARPIN and G. MOUGIN, *Ann. Chim. Fr.* **3** (1978) 305.
5. H. NAONO and R. FUJIWARA, *J. Colloid Interface Sci.* **73** (1980) 406.
6. F. WATARI, J. V. LANDUYT, P. DELAVIGNETTE, S. AMELINCKS and N. IGATA, *Phys. Status Solidi (a)* **73** (1982) 215.
7. P. H. DUVIGNEAUD and R. DERIE, *J. Solid State Chem.* **34** (1980) 323.
8. T. YAMAGUCHI and T. TAKAHASHI, *J. Amer. Ceram. Soc.* **65** (1982) C(83).
9. J. LIMA de FARIA and P. GAY, *Mineral. Magn.* **33** (1962) 37.
10. J. LIMA de FARIA, *Z. Kristallogr.* **119** (1963) 176.
11. K. NAKAJIMA, Y. HIROTSU and S. OKAMOTO, *J. Amer. Ceram. Soc.* **70** (1987) 321.
12. H. P. KLUG and L. E. ALEXANDER, in "X-ray diffraction procedures for polycristalline and amorphous materials" (Wiley, New York, 1974).
13. G. M. da COSTA, E. GALVÃO da SILVA and M. F. de JESUS FILHO, *Hyperfine Interactions*, **67** (1991) 501.
14. U. SCHWERTMANN, *Thermochim. Acta* **78** (1984) 39.
15. C. J. GOSS, *Mineral. Magn* **51** (1987) 437.
16. E. PATTERSON and R. SWAFFIELD, *J. Therm. Anal.* **18** (1980) 161.
17. S. GONI-ELIZALDE and E. GARCIA-CLAVEL, *Thermochim. Acta* **124** (1988) 359.
18. L. G. BERRY, in "Selected powder diffraction data for minerals" (JCPDS, PA, 1974) pp. 365, 533.
19. J. M. FRIEDT, G. K. SHENOY, G. ABSTREITER and R. POINSOT, *J. Chem. Phys.* **59** (1973) 3831.
20. J. M. FRIEDT, M. F. de JESUS FILHO and J. P. SANCHES, *Phys. Status Solidi (b)* **102** (1980) 373.
21. J. D. ARTMAN, A. H. MUIR and H. WIEDERSICH, *Phys. Rev.* **173** (1968) 337.
22. F. WATARI, J. V. LANDUYT, P. DELAVIGNETTE and S. AMELINCKS, *J. Solid State Chem.* **29** (1979) 137.
23. F. WATARI, P. DELAVIGNETTE and S. AMELINCKS, *ibid.* **29** (1979) 417.

Received 2 September 1991
and accepted 17 February 1992